

Ultrastructure of Leaves in *C₄ Cyperus iria* and *C₃ Carex siderosticta*

In Sun Kim^{1*}, Jae-Hong Pak², Bong-Bo Seo², and Seung-Dal Song²

¹Department of Biology, Keimyung University, Taegu 704-701, Korea

²Department of Biology, Kyungpook National University, Taegu 702-701, Korea

The ultrastructural aspects of *Cyperus iria* leaves showing the *C₄* syndrome and the typical *C₃* species, *Carex siderosticta*, in the Cyperaceae family were examined. *C. iria* exhibited the chlorocyperoid type, showing an unusual Kranz structure with vascular bundles completely surrounded by two bundle sheaths. The cellular components of the inner Kranz bundle sheath cells were similar to those found in the NADP-ME *C₄* subtype, having centrifugally arranged chloroplasts with greatly reduced grana and numerous starch grains. Their chloroplasts contained convoluted thylakoids and a weakly-developed peripheral reticulum, although it was extensive mostly in mesophyll cell chloroplasts. The outer mestome bundle sheath layer was sclerenchymatous and generally devoid of organelles, but had unevenly thickened walls. Suberized lamellae were present on its cell walls, and they became polylamellate when traversed by plasmodesmata. Mesophyll cell chloroplasts showed well-stacked grana with small starch grains. In *C. siderosticta*, vascular bundles were surrounded by the inner mestome sheath and the outer parenchymatous bundle sheath with intercellular spaces. The mestome sheath cells degraded in their early development and remained in a collapsed state, although the suberized lamellae retained polylamellate features. Plastids with a crystalline structure, sometimes membrane-bounded, were found in the epidermal cells. The close interveinal distance was 35-50 μm in *C. iria*, whereas it was 157-218 μm in *C. siderosticta*. These ultrastructural characteristics were discussed in relation to their photosynthetic functions.

Keywords: *C₃ Carex siderosticta*, *C₄ Cyperus iria*, Cyperaceae, Kranz anatomy, Leaf ultrastructure, mestome sheath

One of the three photosynthetic pathways, *C₃*, *C₄*, and CAM, occurs among higher plants. The *C₃* pathway is the most common and primitive, and the *C₄* pathway and CAM are considered to be derived and more recent (Ehleringer and Monson, 1993). The taxonomic distribution of the *C₄* species indicates that the *C₄* pathway has evolved numerous times independently among 18 plant families (Dengler and Nelson, 1999). It is also known that plants of different photosynthetic pathways exhibit distinct structural, biochemical, and physiological characteristics (Nelson and Langdale, 1992).

Most plants use the *C₃* photosynthetic pathway, and *C₃* plants have a single cell type, mesophyll cells (MCs), that fix atmospheric CO₂. The *C₄* pathway is a complex adaptation of the *C₃* pathway, and *C₄* plants have two chloroplast types which are found in the bundle sheath cells (BSCs) and MCs. Leaves of *C₄* plants differ in their anatomy from those of *C₃* plants; the BSCs surround each vein, and MCs are radially arranged around the BSCs. *C₄* photosynthesis is also characterized by short interveinal distances as compared with *C₃* leaves (Brown, 1977; Li and Jones,

1994). Thus, the anatomical features of leaves seem to be very important in speculating the phylogenetic relationships between *C₃* and *C₄* species (Takeda et al., 1985). It is suggested that four anatomical features are regarded to be essential for the operation of the *C₄* pathway: 1) structural specialization of BSCs and MCs, 2) positioning of these cells in relation to the vein, 3) a short transport pathway between the two cell types, and 4) structural modification of BSC walls to minimize the apoplastic CO₂ leakage (Soros and Dengler, 1998; Dengler and Nelson, 1999). Depending on differences in their decarboxylation systems, *C₄* plants are divided into three biochemical subtypes: NADP-ME, NAD-ME, and PEP-CK (Hatch, 1987). These biochemical distinctions are correlated with the ultrastructural differences of the BSCs (Ueno et al., 1988; Dengler and Nelson, 1999). Thus, the compartmentalization of activities into two specialized cells and their chloroplast types are the key features of *C₄* photosynthesis (Furbank and Taylor, 1995; Ueno, 1996; Dengler and Nelson, 1999). In studies of the *C₄* Cyperaceae leaf structure, the terms Kranz sheath cells (KCs) have been commonly used in place of inner BSCs, and mestome sheath cells (MST) for in place of outer BSCs (Carolin et al., 1977; Takeda et al., 1980; Ueno et al., 1986, 1988; Ueno, 1996; Soros and Den-

*Corresponding author; fax 82-53-580-5164
e-mail botany@kmucc.keimyung.ac.kr

gler, 1998; Dengler and Nelson, 1999). Accordingly, we have used this terminology throughout the study.

Among monocot families, except Poaceae, the Cyperaceae includes the largest number of C_4 species (Takeda et al., 1985; Bruhl and Perry, 1995; Soros and Dengler, 1998). There are considerable distinctions in anatomical, ultrastructural, and biochemical features among species within the Cyperaceae. Correlations between C_4 subtypes and features of BSCs have long been known within the family (See Dengler and Taylor, 1999). Based on several anatomical features, four Kranz anatomical types have been recognized (Ueno et al., 1988; Ueno and Samejima, 1989; Soros and Dengler, 1998; Dengler and Nelson, 1999). The ultrastructure of C_4 cyperaceous species, in relation to biochemistry, has been investigated much more than that of C_3 species. Features of the internal foliar structure in C_3 cyperaceous species have received little attention, although some *Carex* have been studied micromorphologically (Standley, 1990; Waterway, 1990). In this study, we examined the foliar structural characteristics of C_4 and C_3 species in Cyperaceae plants that commonly occur in Korea. *Carex siderosticta* was used as a C_3 species and *Cyperus iria* as a C_4 species for its known biochemical features (Ueno et al., 1986; Ueno and Takeda, 1992). The purpose of this study is to compare the leaf ultrastructures of C_4 *C. iria* and a typical C_3 *C. siderosticta*, and to evaluate the structural features in relation to C_4 and C_3 photosynthesis.

MATERIALS AND METHODS

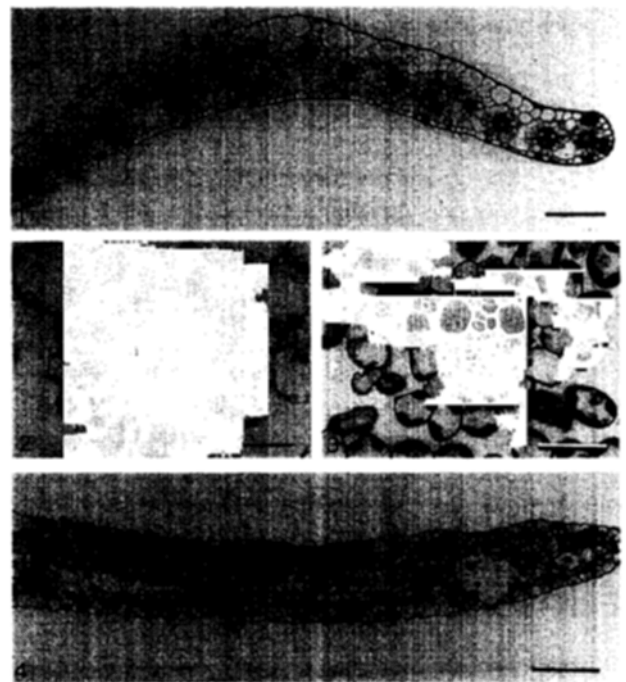
Approximately ten plants of each *C. iria* L. and *C. siderosticta* Hance, classified according to Oh (1994), were collected from the low lands of the Kyungsang Province during 1997-1998. Most plant leaves were used immediately for tissue sampling during and/or after field collection, but the others were transferred to a growth chamber, where they were maintained throughout the study. In both species, the median parts of fully expanded mature blades were sampled for electron microscopy. The leaf tissues were prepared according to Kim et al. (1997, 1998). The fixed tissues were washed four times in the same buffer and postfixed in 2% osmium tetroxide for 2 h to overnight at 4°C. These tissues were then washed several times in the buffer before dehydration with a graded acetone or alcohol series. The specimens were embedded in Spurr's low viscosity resin after substitution and infiltration. Ca. 0.5-1 μm thick transverse

sections were made on a Reichert RMC 6000 ultramicrotome either using a histo-diamond knife or glass knives. The sections were stained with toluidine blue O and photographed with a Zeiss Polyvar microscope. Approximately 60-90 nm ultrathin sections were cut with a diamond knife. Sections on the copper grids coated with 0.35% formvar in dichloroethane were stained with 2% aqueous uranyl acetate and lead citrate for 30-45 min. Sections were rinsed three to four times with filtered 50% ethanol and with filtered CO_2 -free water and examined with a Hitachi H-7100 electron microscope at the Korea Basic Science Institute, Taegu Branch.

RESULTS

Anatomy

From a cross-sectional view, it was observed that



Figures 1-4. Light micrographs of leaf cross sections in *C. iria* and *C. siderosticta*. **1.** Part of a *C. iria* leaf. The mid vein is not shown here. Scale = 100 μm . **2.** Closeup of a vein in *C. iria* showing the Kranz bundle sheath (a), mestome sheath (b), and mesophyll cells (c). Scale = 45 μm . **3.** Closeup of a minor vein in *C. siderosticta* showing a degraded mestome sheath (a), parenchymatous bundle sheath (b), and mesophyll cells (c). Scale = 100 μm . **4.** Part of a *C. siderosticta* leaf. Scale = 80 μm . Note the considerable difference of the interveinal distance between the two species in Figure 1 and Figure 4.

C. iria contained small and numerous vascular bundles that were surrounded completely by the inner and outer bundle sheaths. The inner bundle sheath cells contained conspicuous chloroplasts, whereas the outer ones were sclerenchymatous and appeared empty (Figs. 1 and 2). The interveinal distance (IVD) was ca. 35-50 μm . A group of inflated bulliform cells were located at the middle of the adaxial epidermis. In the flat leaves of *C. siderosticta*, vascular bundles were surrounded by two layers of bundle sheath cells: inner sheath cells were collapsed and sclerenchymatous, and outer ones were parenchymatous and various in size. Thus, these leaves showed a non-

Kranz anatomy. Intercellular spaces were huge between bundles and the IVD was ca. 157-218 μm in this species (Figs. 3 and 4). In both species, the upper epidermal cells were larger than the lower epidermal cells. The stomata were abaxial, and guard cells were positioned at the level of the epidermal surface.

Ultrastructure

Leaves of *C. iria* exhibited a modified Kranz anatomy in which the chlorenchymatous KCs were almost always separated from the rest of the MCs by a layer of MST cells (Fig. 5). No intercellular spaces were



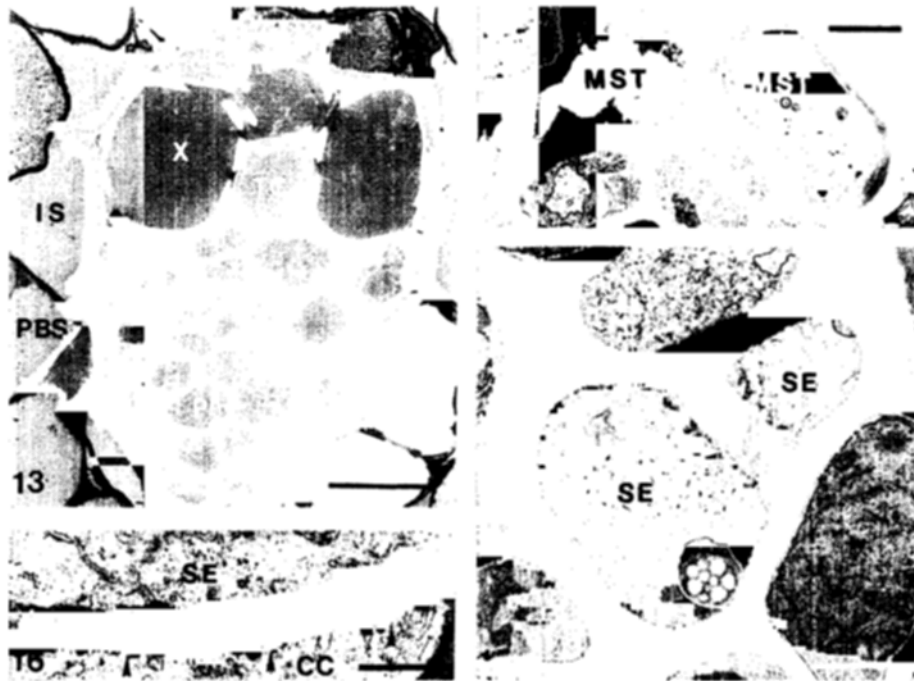
Figures 5-8. Electron micrographs of *C. iria* leaf cross-sectioned. **5.** Vascular bundle and its sheath showing Kranz anatomy. Two bundle sheath layers, consisted of the inner Kranz bundle sheath (KC) and mestome sheath (MST), enclose the vascular bundle (VB). A tannin cell (TC) is formed in the inner KC layer. IS = intercellular space, MC = mesophyll cell. Scale = 10 μm . **6.** A KC containing two chloroplasts (C) with several starch grains (S). The mestome sheath cells appear empty. Scale = 2 μm . **7.** The junction of a KC and two MST cells. Note the striation in the KC wall (arrow) and polylamellate suberized lamellae (SL) on the MST cell walls (Insert, scale = 100 μm). The SL do not fuse in the radial walls (arrow heads). W = cell wall. Scale = 1 μm . **8.** Frequent plasmodesmata connections (arrows) between the KC and MST cells, and between the MC and MST cells. As a KC becomes a tannin cell (TC), its cell wall becomes thinner than that of the KC. Scale = 2 μm .

observed between the cells of vascular tissues and the inner and outer bundle sheaths. Organelles in the KCs were arranged either centrifugally or occupied the cytoplasm entirely. Each KC had a count of one or two chloroplasts per cell section. These chloroplasts were large and contained several starch grains (Fig. 6). The chloroplasts contained convoluted thylakoids which occupied most of the stroma region. The KC chloroplasts also had peripheral reticulum (PR) vesicles that weakly extended to the margins of the chloroplasts. Mitochondria in these KCs were rather small as in the MCs, but no significant increase in size and number was noticed. The MST cells, tightly encir-

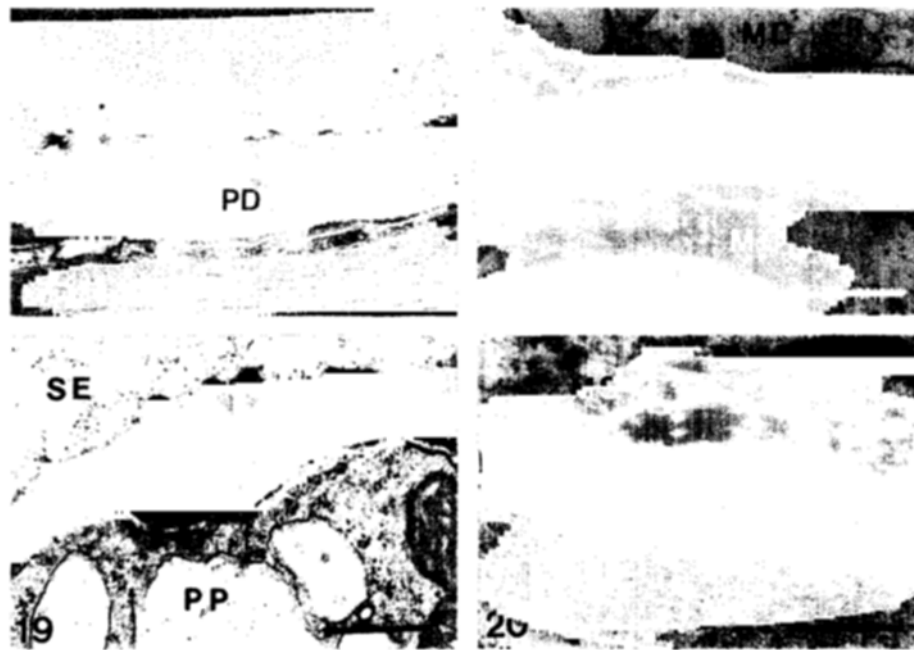
cling the KCs, were small and possessed little cytoplasm and unevenly thickened cell walls. The radial walls of the MST cells were shorter than the tangential walls and exhibited a suberized lamellae (SL) structure (Fig. 7). Plasmodesmata were most frequent between MST cells and KCs and between MST and MCs, but they were not observed between KCs and neighboring vascular cells. The plasmodesmata connections were restricted in the pit fields (Fig. 8), where the SL showed a distinct polylamellate appearance (Fig. 7, Insert). Plasmodesmata were constricted when they traversed the SL. However, no such constriction appeared between KCs or between MCs.



Figures 9-12. Electron micrographs of mesophyll cells in *C. iria* and *C. siderosticta* leaves. **9.** Radially arranged mesophyll cells (MCs), part of a mestome sheath (MST), and an epidermal cell (E) of *C. iria*. Tannin is accumulating in an MC₁. IS = intercellular space. Scale = 5 μ m. **10.** Closeup of the peripheral reticulum (PR) with anastomosing electron transparent vesicles in *C. iria*. C = chloroplast, S = starch grain. Scale = 0.5 μ m. **11.** Transverse section of a partial vein in *C. siderosticta*: parenchymatous bundle sheath (PBS) cells are external to the mestome sheath (MST) cells and surrounded by large MCs. F = sclerenchyma fiber. Scale = 5 μ m. **12.** Numerous mitochondria (m) and microbodies (mb) are visible among MC chloroplasts of *C. siderosticta*. Scale = 3 μ m.



Figures 13-16. Electron micrographs of *C. siderosticta* leaves. **13.** A cross-section showing a vascular bundle consisting of the xylem (X), phloem (Ph), xylem parenchyma (XP), and a tannin cell (TC) and bundle sheath. The bundle sheath consists of two layers: the inner collapsed sheath and the outer parenchymatous sheath. Scale = 5 μm . **14.** Intact mestome sheath (MST) cells. No intercellular space is observed between them. Scale = 2 μm . **15.** A plastid with crystalloids in the sieve element (SE). The arrow indicates the sieve plate. Scale = 1 μm . **16.** Numerous plasmodesmata (arrowheads) between a sieve element (SE) and companion cell (CC). Scale = 0.5 μm .

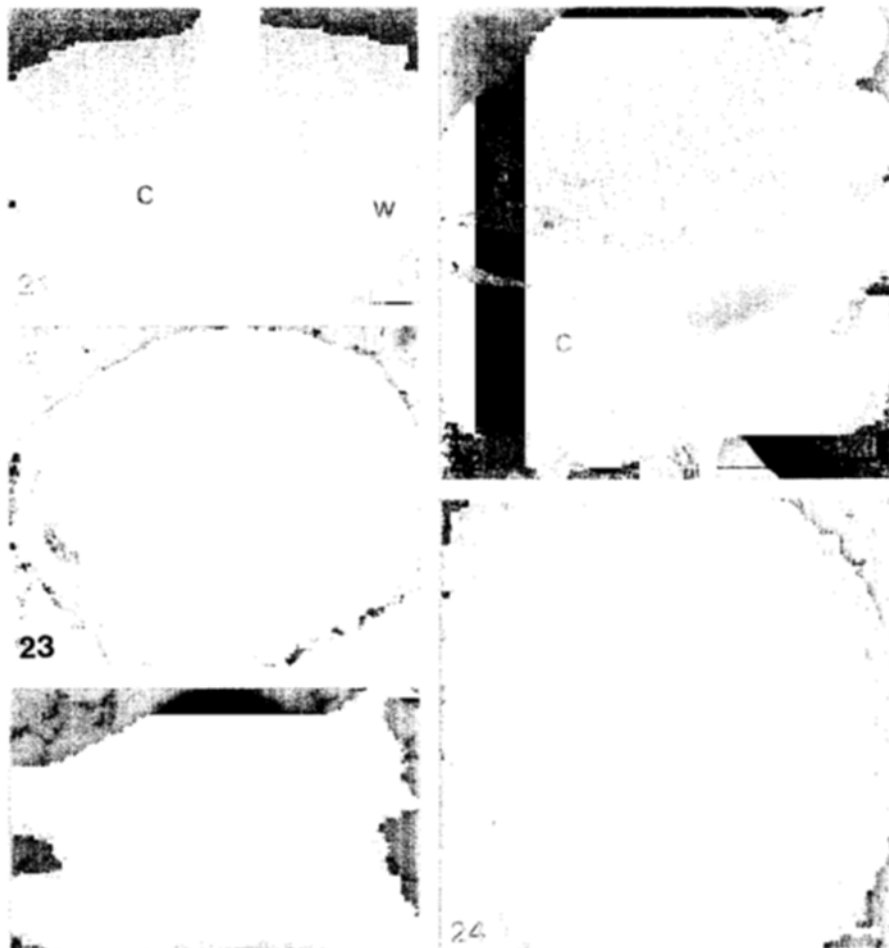


Figures 17-20. Plasmodesmata in *C. siderosticta*. All scales equal to 0.4 μm . **17.** Plasmodesmata (PD) between an epidermal cell (E) and a mesophyll cell (MC). **18.** Plasmodesmata between two adjacent MCs. **19.** Peculiarly formed plasmodesmata (arrow) between a phloem parenchyma cell (PP) and a sieve element (SE). **20.** A cell wall (W) interfaces between the degrading mestome sheath (MST) cell and an MC. Note the SL and plasmodesmata constrictions. The SL layer slightly widens and becomes polylamellate where the plasmodesmata transverse.

The MCs were displaced radially around the MST cells, and huge intercellular spaces were formed among them (Fig. 9). Tannin cells developed frequently from the vascular parenchyma, KCs, and MCs (Figs. 5, 8, and 9). When these cells transformed into tannin cells, their cell walls became very thin (Fig. 8). Chloroplasts in the MCs were mostly of oval or lenticular shape and possessed small starch grains, numerous well-developed grana, and a PR. The PR had developed highly in the MC chloroplasts and formed arrays of vesicles or anastomosing tubules at the periphery of the stroma (Fig. 10).

Leaves of *C. siderosticta* revealed typical non-Kranz anatomy, having two layers of sheaths composed of an inner collapsed MST, an outer parenchymatous

bundle sheath (PBS), and MCs of somewhat random arrangement. The large intercellular spaces were developed between the MCs (Fig. 11). The outer PBS cells, especially on the xylem and phloem side, were smaller in size than the MCs, but their chloroplasts were similar in size and structure to those found in the MCs. Many MCs contained dense cytoplasm including mitochondria and microbodies (Fig. 12). Irregularly shaped MC chloroplasts with protuberances consisting entirely of stroma also occurred frequently. The inner MST cells in *C. siderosticta* degraded in their early development and remained in a collapsed state throughout their development (Fig. 13), resulting in huge intercellular spaces between the MST and PBS and between the MST and some vasc-



Figures 21-25. Electron micrographs of plastids in the epidermal cells of *C. siderosticta*. **21.** Guard cells (GC) in a stoma showing chloroplasts with starch grains and reduced grana. Scale = 2 μm . **22.** Different size and structure of plastids (P) between an epidermal cell (E) and mesophyll cells (MCs). N = nucleus. Scale = 2 μm . **23.** A triangular crystalline structure (CR), peripheral reticulum (PR, arrowheads), and plastoglobuli (arrows) in a plastid. Scale = 0.4 μm . **24.** A plastid with a serrate membrane-bounded crystalline structure. The arrow indicates the trace of PR. PE = plastid envelope. Scale = 0.2 μm . **25.** A plastid with a few irregular single thylakoids (arrowhead), plastoglobuli (arrow) and crystalline structure. Scale = 5 μm .

ular parenchyma cells. However, no intercellular spaces were found between the intact normal MST cells (Fig. 14). Vascular parenchyma cells adjacent to the MST were small to medium in size and contained moderately dense cytoplasm and thick walls. Tannin substance was also accumulated in the vacuoles of the MCs, PBS cells and vascular parenchyma cells (Fig. 13). Within the vascular tissues, xylem elements tended to be developed earlier than phloem elements. Sieve elements contained P-type plastids with protein crystalline structures (Fig. 15). Plasmodesmata between sieve element and companion cells were numerous (Fig. 16), but in general they were rather simple in structure and few in number at the interfaces among the MST cells, PBS cells, MCs, vascular cells, and epidermal cells (Figs. 17 and 18). They did not, however, exhibit such characteristics among cells in the phloem (Fig. 19). An SL structure was present in the collapsed MST cell wall neighboring the vascular parenchyma and the MCs (Fig. 20). Plasmodesmata were constricted where they traversed slightly widened SL. The plastids of the epidermal cells and guard cells of *C. siderosticta* differed in number, structure, and size in comparison to those of *C. iria*. Plastids in the guard cells were similar to the amyloplast having starch grains and very reduced grana (Fig. 21). Plastids in the epidermal cells were usually smaller than plastids found in other cell types (Fig. 22). They contained crystalline lattice structures, PR or PR-like vesicles, and plastoglobuli (Fig. 23). Many crystalline structures were bounded by serrate membranes (Fig. 24). The subunits of the crystalline structure appeared to be regularly arranged. The plastids usually did not contain any thylakoid system, but a few irregularly arranged single thylakoids were rarely found (Fig. 25).

DISCUSSION

The KCs of *C. iria* showed characteristics of the foliar ultrastructure reported for the chlorocyperoid NADP-ME type of the Cyperaceae. In this species, the PR in chloroplasts was weakly developed in the KCs and well-developed in the MCs. Contrasting to the present study, a highly developed PR was found in the KC chloroplasts in the studies of *Cyperus victoriensis* (Carolin et al., 1977) and *Cyperus longus* (Jones et al., 1981). In our study, the PR, often observed in the KC chloroplasts, did not appear to be organized in the same manner as that in the MC chloroplasts. The functional significance of the PR is not completely understood, but is thought to facilitate the transfer of

metabolites across the chloroplast envelope (Laetsch, 1971; Ueno et al., 1988). The KCs exhibited almost centrifugally arranged large chloroplasts. Features of KCs such as chloroplasts with agranal convoluted thylakoids and mitochondria showing no significant increase in number and size were frequently observed as they were in other chlorocyperoid species (Laetsch, 1974; Carolin et al., 1977; Ueno et al., 1988). The KCs formed a complete sheath on the side of the MST in smaller bundles, but in large bundles, the MST was interrupted by the metaxylem element. The arrangement of the vascular tissue and the remaining chlorophyllous parenchyma in *C₄* Cyperaceae has been considered abnormal due to the presence of a layer of non-chlorophyllous MST cells between the KCs and MCs (Takeda et al., 1980; Soros and Dengler, 1998). The KCs are usually characterized by thicker walls, numerous pit fields and plasmodesmata, and their chloroplast shape, size, frequency, and specific position within each cell (Brown, 1977; Ueno et al., 1988; Dengler and Nelson, 1999). Hattersley and Browning (1981) have suggested that the centrifugally arranged chloroplasts reduce the diffusion path length for intermediate metabolites of the *C₄* pathway, thus enhancing photosynthetic efficiency.

Regulation of chloroplast numbers per cell, chloroplast enlargement, elaboration of internal membranes to form grana and PR, and expression and activity of starch synthetic pathways are important factors for *C₄* development (Dengler and Nelson, 1999). In the Cyperaceae, the SL always occupied the inner and outer tangential walls of the MST cells (Soros and Dengler, 1998). The SL structure is believed to consist of the suberin polymer and other substances that are relatively impermeable to water (Hattersley and Browning, 1981). Accordingly, the distribution of SL in the MST cells of *C₄* Cyperaceae is of particular interest in relation to *C₄* photosynthetic metabolism. Species having an MST layer may be under higher resistance to the transport of photosynthates to the phloem than species without an MST layer. The reason for this is evident, as the KCs are separated from the MCs or PBS by MST cells with thick walls, while in the species without the MST layer the KCs are in direct contact with MCs or PBS cells (Ueno et al., 1988). Thus, the access of CO₂ to KC chloroplasts is complicated by the presence of a suberin layer in the MST cell wall (Laetsch, 1971; Dengler and Nelson, 1999). The function of the non-photosynthetic MST cells is not yet clearly understood, but their role as an additional physiological barrier to the transport of metabolites (Chen et al., 1974; Hattersley and

Browning, 1981; Ueno et al., 1988) and their role in maintaining high CO₂ concentration in the KCs (Ueno and Samejima, 1989) have been suggested.

In C₃ species, MCs are the primary site of photosynthesis, and the parenchymatous sheath cells are not specialized as seen in the leaves of *C. siderosticta*. A PBS layer was located between the MST cells and MCs. A PBS layer is present in C₃ cyperaceous species, but its presence in the C₄ cyperaceous species is known to be variable (Soros and Dengler, 1998). When present in C₄ species, the PBS layer appears to function as MCs (Soros and Dengler, 1998; Dengler and Nelson, 1999). In this study, the PBS usually had fewer and smaller chloroplasts, while more cellular components were often observed in the MCs. Unlike typical C₃ MC chloroplasts, many MC chloroplasts in *C. siderosticta* were quite irregular in shape, with traces of PR-like vesicles. The MCs in this C₃ *Carex* were not different from MCs in the C₄ *Cyperus* examined, but the latter exhibited radially elongated MCs in which such an arrangement permitted each cell to tighten its contact with the outer tangential walls of the MST cells. In *C. iria*, the KCs were not large in size compared to the PBS of *C. siderosticta*, but the former had large and numerous chloroplasts with some starch grains and a centrifugal arrangement of cytoplasmic components. In leaves of *C. iria*, most of the KCs were associated with numerous small veins. The associations of the KCs with small veins probably play a role in maintaining the CO₂ concentrating mechanism that results in a more efficient photosynthetic performance (Li and Jones, 1994). The mean IVD value previously reported among C₄ *Cyperus* species ranges from 38 to 126 μm (Takeda et al., 1980; Li and Jones, 1994), while the value in C₃ species ranges from 168 to 324 μm (Takeda et al., 1980; Li and Jones, 1994). Estimates of the IVD in this study well fell into those ranges. The IVD is one of the most reliable features in assessing C₄ anatomy (Li and Jones, 1994). A short IVD in C₄ leaves indicates that assimilate transport toward phloem cells from the MCs may be more direct, rapid, and efficient when compared to that of C₃ leaves (Rao and Rajendrudu, 1989; Li and Jones, 1994; Dengler and Taylor, 1999). It has been suggested that the C₄ pathway has evolved from the C₃ photosynthesis on a number of occasions, and this hypothesis has been supported by several approaches (See Sage and Monson, 1999).

The Kranz anatomy of C₄ leaves is believed to be achieved by the modification of the developmental process of the C₃ ancestral type, especially by the alteration of the leaf venation pattern, position of KCs

and MCs in relation to leaf veins, cell-specific expression of photosynthetic enzymes, and structural features of cells (Dengler and Nelson, 1999). The reduction of bundle sheath layers, as in the chlorocyperoid species, probably provides advantages to the smooth exchange of photosynthates between MCs and KCs (Takeda et al., 1985). The assumed anatomical evolutionary process from the non-Kranz C₃ type to the Kranz C₄ type in the Cyperaceae has been proposed by Ueno et al. (1989). According to their assumption, the most primitive type would be the non-Kranz type with small vascular parenchyma cells (NK-S) and the evolutionary process has probably undergone the following steps: NK-S → NK-M → NK-L → Intermediate → Kranz-like → several C₄ subtypes. NK-M and NK-L refer to the non-Kranz types with vascular parenchyma cells of medium and large size, respectively. Some C₃ cyperaceous species have an outer layer of xylem and phloem parenchyma that contain small chloroplasts, and KCs in the C₄ Cyperaceae, especially of the chlorocyperoid type, are believed to have originated from the vascular parenchyma cells (Brown, 1975; Carolin et al., 1977; Ueno et al., 1989; Ueno and Takeda, 1992; Ueno, 1996). Some degree of modification of the KCs and MCs, as shown in Figures 5, 8, 9, and 13, were well noticed in tannin-forming cells of both *C. iria* and *C. siderosticta* during the study. When tannin cells, presumably for deterring herbivores (Ehleringer and Monson, 1993), were formed from various cells such as the KC, MC, and xylem parenchyma, the cells enlarged considerably with very thin cell walls. If such structural modification takes place in the cells adjacent to the vascular tissue near the MST layer in C₃ species, with the necessary programmed genetic information, there exists the possibility of cell transformation into other cell types such as the KCs or MST cells. It is conceivable that an ancestral C₄-like or C₄ structure may be originated through transformation process. Therefore, an extensive research on the development and structure of the C₄ leaf and closely related C₃ taxa should be carried out for a better understanding of the C₃ and C₄ structural relationships.

ACKNOWLEDGEMENTS

The present study was supported by the Basic Science Research Institute Program, 1997, Ministry of Education in Korea Project No. BSRI-97-4404.

Received May 3, 1999; accepted July 23, 1999.

LITERATURE CITED

- Brown WV (1975) Variations in anatomy, associations, and origins of Kranz tissue. *Amer J Bot* 62: 395-402
- Brown WV (1977) The Kranz syndrome and its subtypes in grass systematics. *Mem Torr Bot Club* 23: 1-97
- Bruhl J, Perry S (1995) Photosynthetic pathway-related ultrastructure of C₃, C₄ and C₃-like and C₃-C₄ intermediate sedges (Cyperaceae), with special reference to *Eleocharis*. *Aust J Plant Physiol* 22: 521-530
- Carolin RC, Jacobs SWL, Vesk M (1977) The ultrastructure of cells of the mesophyll and parenchymatous bundle sheath of the Gramineae. *Bot J Linn Soc* 66: 259-275
- Chen TM, Dittrich P, Campbell WH, Black CC (1974) Metabolisms of epidermal tissues, mesophyll cells, and bundle sheath strands resolved from mature nutsedge leaves. *Arch Bioch Bioph* 163: 246-262
- Dengler NG, Nelson T (1999) Leaf structure and development in C₄ plants. In RF Sage, RK Monson, eds, C₄ Plant Biology, Academic Press, New York, pp 133-172
- Ehleringer JR, Monson RK (1993) Evolutionary and ecological aspects of photosynthetic pathway variation. *Annu Rev Ecol Syst* 24: 411-439
- Furbank RT, Taylor WC (1995) Regulation of photosynthesis in C₃ and C₄ plants: a molecular approach. *Plant Cell* 7: 797-807
- Hatch MD (1987) C₄ photosynthesis: a unique blend of modified biochemistry, anatomy and ultrastructure. *Bioch et Biophys Acta* 895: 81-106
- Hattersley PW, Browning AJ (1981) Occurrence of the suberized lamella in leaves of grasses of different photosynthetic types. I. In parenchymatous bundle sheaths and PCR ("Kranz") sheaths. *Protoplasma* 109: 371-401
- Jones MB, Hannon GE, Coffey MD (1981) C₄ photosynthesis in *Cyperus longus* L., a species occurring in temperate climates. *Plant Cell and Environment* 4: 161-168
- Kim IS, Pak JH, Seo BB, Song SD (1997) Ultrastructural aspects of Kranz anatomy in *Digitaria sanguinalis* and *Setaria viridis* (Poaceae). *J Plant Biol* 40: 102-109
- Kim IS, Pak JH, Seo BB, Song SD (1998) Ultrastructural aspects of leaves in *Festuca ovina* and *Poa sphondylodes* (C₃ Poaceae). *J Plant Biol* 41: 170-177
- Laetsch WM (1971) Chloroplast structural relationships in leaves of C₄ plants. In MD Hatch, CB Osmond, RO Slayter, eds, Photosynthesis and Photorespiration, Wiley Interscience, New York, pp 323-349
- Laetsch WM (1974) The C₄ syndrome: a structural analysis. *Ann Rev Plant Physiol* 25: 27-52
- Li M, Jones MB (1994) Kranzkette, a unique C₄ anatomy occurring in *Cyperus japonicus* leaves. *Photosynthetica* 30: 117-131
- Nelson T, Langdale JA (1992) Developmental genetics of C₄ photosynthesis. *Annu Rev Plant Physiol Plant Mol Biol* 43: 25-47
- Oh YC (1994) Manual of the Korean Cyperaceae. Vol II. Sungshin Womans University Press, Seoul, pp 23-59
- Rao AP, Rajendrudu G (1989) Net photosynthetic rate in relation to leaf anatomical characteristics of C₃, C₃-C₄ and C₄ dicotyledons. *Proc Indian Acad Sci* 99: 529-537
- Sage RF, Monson RK (1999) C₄ Plant Biology. Academic Press, New York, pp 3-596
- Soros CL, Dengler NG (1998) Quantitative leaf anatomy of C₃ and C₄ Cyperaceae and comparisons with the Poaceae. *Int J Plant Sci* 159: 480-491
- Standley LA (1990) Anatomical aspects of the taxonomy of sedges (*Carex*, Cyperaceae). *Can J Bot* 24: 1449-1456
- Takeda T, Ueno O, Agata W (1980) The occurrence of C₄ species in the genus *Rhynchospora* and its significance in Kranz anatomy of the Cyperaceae. *Bot Mag* 93: 55-65
- Takeda T, Ueno O, Samejima M, Ohtani T (1985) An investigation for the occurrence of C₄ photosynthesis in the Cyperaceae from Australia. *Bot Mag* 98: 393-411
- Ueno O (1996) Structural characterization of photosynthetic cells in an amphibious sedge, *Eleocharis vivipara*, in relation to C₃ and C₄ metabolism. *Planta* 199: 382-393
- Ueno O, Samejima M (1989) Structural features of NAD-malic enzyme type C₄ *Eleocharis*: an additional report of C₄ acid decarboxylation types of the Cyperaceae. *Bot Mag* 102: 393-402
- Ueno O, Samejima M, Koyama T (1989) Distribution and evolution of C₄ syndrome in *Eleocharis*, a sedge group inhabiting wet and aquatic environments, based on culm anatomy and carbon isotope ratios. *Ann Bot* 64: 425-438
- Ueno O, Takeda T (1992) Photosynthetic pathways, ecological characteristics, and the geographical distribution of the Cyperaceae in Japan. *Oecologia* 89: 195-203
- Ueno O, Takeda T, Murata T (1986) C₄ acid decarboxylating enzyme activities of C₄ species possessing different Kranz anatomical types in the Cyperaceae. *Photosynthetica* 20: 111-116
- Ueno O, Takeda T, Maeda E (1988) Leaf ultrastructure of C₄ species possessing different Kranz anatomical types in the Cyperaceae. *Bot Mag* 101: 141-152
- Waterway M (1990) Systematic implications of achene micromorphology in *Carex* section *Hymenochlaena* (Cyperaceae). *Can J Bot* 68: 630-639